

## Determining ionizing radiation using sensors based on organic semiconducting material

Harshil N. Raval,<sup>a)</sup> Shree Prakash Tiwari, Ramesh R. Navan, and V. Ramgopal Rao<sup>b)</sup>

Department of Electrical Engineering, Centre for Nanoelectronics, Indian Institute of Technology, Bombay 400 076, India

(Received 11 December 2008; accepted 6 March 2009; published online 26 March 2009)

The use of organic semiconducting material sensors as total dose radiation detectors is proposed, wherein the change in conductivity of an organic material is measured as a function of ionizing radiation dose. The simplest sensor is a resistor made using organic semiconductor. Furthermore, for achieving higher sensitivity, organic field effect transistor (OFET) is used as a sensor. A solution processed organic semiconductor resistor and an OFET were fabricated using poly 3-hexylthiophene (P3HT), a *p*-type organic semiconductor material. The devices are exposed to Cobalt-60 radiation for different total dose values. The changes in electrical characteristics indicate the potential of these devices as radiation sensors. © 2009 American Institute of Physics. [DOI: 10.1063/1.3107266]

Operational performance of electronic devices degrades with their exposure to ionizing radiation.<sup>1,2</sup> Radiation effects are a grave concern for space environment, nuclear applications, and electronics gadgets operating in radiation environment. In metal oxide semiconductor (MOS) devices, total dose effects affect the gate dielectric. Defects generated in dielectric cause charge trapping, mobility degradation, shift in the operating voltages, and increased power dissipation in the devices.<sup>2</sup> These radiation effects can be used to build sensors for radiation dosimetry.<sup>3</sup> Use of *p*-type MOS transistor in dosimeter was demonstrated by experiments on Explorer-55.<sup>1</sup> MOS dosimeters are used in the spacecraft, radiation therapy, and personal dosimetry.<sup>3</sup>

The use of organic semiconducting materials is well known for making organic light emitting diodes (OLEDs), organic photovoltaic cells (OPVs), and organic field effect transistors (OFETs).<sup>4-9</sup> Also, the use of organic semiconductor material is explored for vapor sensing applications and chemical sensing applications,<sup>10,11</sup> as well as various biomedical applications.<sup>12,13</sup> All these devices use various organic semiconducting materials as their active material. An application of using organic semiconductor material sensors for determining ionizing radiation is reported in this work. Ionizing radiation has its applications in the field of medical radiation therapy as a part of cancer treatment, radiation dosimeters for personal dosimetry, and radiation dose control for food preservation applications.

On a silicon wafer with a thick (~500 nm) thermally grown oxide (SiO<sub>2</sub>), interdigitated Ti/Au (10 nm/50 nm) electrodes are patterned using lift-off photolithography technique. Hexamethyldisilazane (HMDS) surface treatment was done by spin coating the HMDS on substrate at 500 rpm for 5 s followed by 4000 rpm for 50 s. The films were annealed at 120 °C for 5 min. P3HT was dissolved in chloroform in a 3 mg/ml weight ratio, heated up to 60 °C, and stirred in ultrasonic bath to form a uniform solution. This solution was then spin coated on the substrate at 500 rpm for 15 s fol-

lowed by 1000 rpm for 40 s to form an organic resistor. The sample was then annealed for 90 min at 90 °C. A schematic top view of the fabricated organic semiconductor resistor sensor is shown in Fig. 1(a).

The organic semiconductor resistor sensor was irradiated using a Cobalt-60 (<sup>60</sup>Co) radiation source. The dose rate provided by the radiation source is 1 krad/min. The sample was irradiated for different doses by varying the time for irradiation. After each irradiation the current-voltage (*I**V*) characteristics of the resistor were measured on a probe station using Keithley 2602 Source-Measure Unit (SMU) at room temperature in the normal atmospheric conditions. A varying dc voltage was applied between the two interdigitated electrodes of the sensor and the current flowing between them

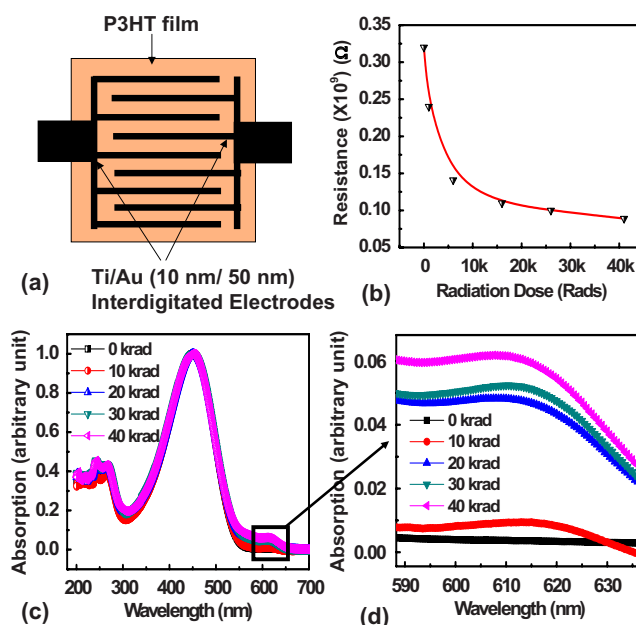


FIG. 1. (Color online) (a) Schematic top-view of an organic semiconductor resistor sensor formed using two interdigitated electrodes covered using a *p*-type organic semiconductor—P3HT film. (b) Change in the resistivity of the sensor with increasing ionizing radiation dose. (c) UV-visible spectrum for the P3HT solution prepared in chloroform and exposed to <sup>60</sup>Co radiation for increasing dose. (d) The oxidation peak in Fig. 1(c), showing increase in oxidizing peak with increasing radiation dose.

<sup>a)</sup> Author to whom correspondence should be addressed. Electronic mail: hnraval@ee.iitb.ac.in. Tel.: +91-22-2576-7456. FAX: +91-22-2572-3707.

<sup>b)</sup> Electronic mail: rrao@ee.iitb.ac.in. Tel.: +91-22-2576-7456. FAX: +91-22-2572-3707.

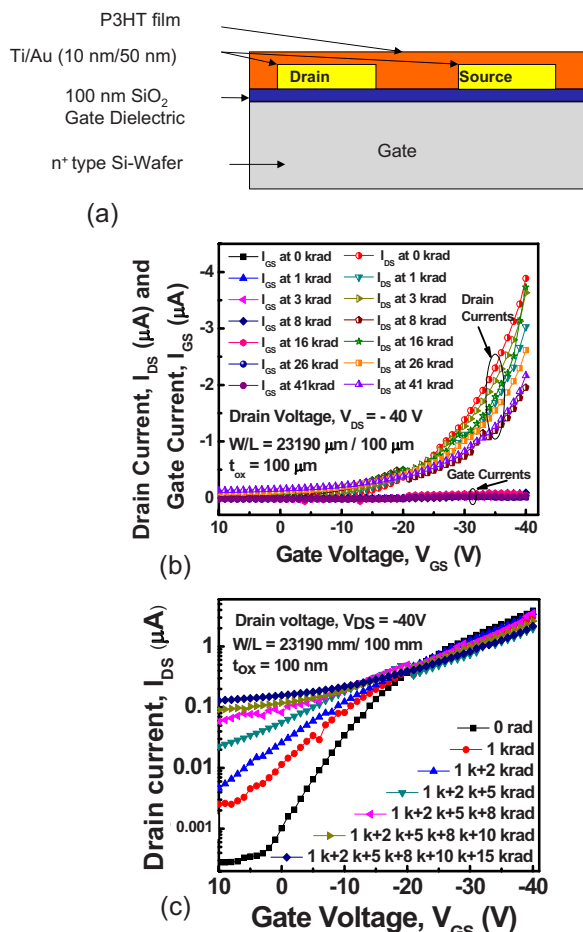


FIG. 2. (Color online) (a) Schematic cross section of a bottom-gate-bottom-contact *p*-type OFET with P3HT as its active material and with  $W/L = 23190 \mu\text{m}/100 \mu\text{m}$  and 100 nm thermally grown  $\text{SiO}_2$  on  $n^+$  silicon wafer as gate dielectric. (b) Change in  $I_{\text{DS}}-V_{\text{GS}}$  characteristics of the OFET with increasing ionizing radiation dose of  $^{60}\text{Co}$ . (c) Showing OFF current and subthreshold degradation ( $\log I_{\text{DS}}$  vs  $V_{\text{GS}}$  plot) for the OFET with increasing ionizing radiation dose of  $^{60}\text{Co}$ .

was measured. As shown in Fig. 1(b), the resistance of the sample decreases with increasing total ionizing radiation dose. The resistance decreases from 320 to 80 M $\Omega$  for a nonirradiated sample to the one irradiated with 41 krad dose. When the P3HT is subjected to high energy  $^{60}\text{Co}$  radiation, the thiophene molecule in the chain of this polymer goes to a polaron state and gets stabilized to a bipolaron and a neutral state and stays in this oxidized state.<sup>14,15</sup> The band gap of P3HT decreases [distance between the highest occupied molecular orbital (HOMO) and lowest unoccupied molecular orbital (LUMO) levels] and the material becomes more conductive. This phenomenon can also be observed in the UV-visible spectroscopy measurements performed on a solution of P3HT prepared in chloroform and subjected to an increasing dose of  $^{60}\text{Co}$  radiation by varying the time of radiation exposure. Figure 1(c) shows the obtained UV-visible spectrum that shows a peak of absorption at 450 nm wavelength for unexposed P3HT solution. Figure 1(d) shows an increasing absorption peak at 610 nm wavelength due to the oxidation of P3HT with increasing radiation. The ionizing radiation study was also performed on bottom-gate-bottom-contact OFET sample, schematic of which is shown in Fig. 2(a). For this, a heavily doped *n*-type silicon substrate with 100 nm thick thermally grown  $\text{SiO}_2$  as the gate dielectric

(capacitance = 34.5 nF/cm<sup>2</sup>) was used for the OFET fabrication. The Ti/Au electrodes (contacts for source drain), HMDS treatment, semiconductor layer formation, and annealing were done as described in the resistor fabrication section. OFETs were characterized on a probe station using Keithley 2602 and Keithley 236 SMUs at room temperature in the normal atmospheric conditions at a relative humidity values less than 20%. For the radiation study involving the organic transistor, the sample was irradiated with a  $^{60}\text{Co}$  radiation source (dose rate is 1 krad/min). The sample was irradiated for different doses by varying the time for irradiation. After each irradiation, the sample was electrically characterized.

Figure 2(b) shows the  $I_{\text{DS}}-V_{\text{GS}}$  characteristics of an OFET with a  $W/L$  ratio of 23 190  $\mu\text{m}/100 \mu\text{m}$ . With no radiation, the device shows  $I_{\text{ON}}/I_{\text{OFF}}$  ratio of  $\sim 3800$  and a mobility of  $\sim 1.7 \times 10^{-3} \text{ cm}^2 \text{ V}^{-1} \text{ s}^{-1}$ . The threshold voltage ( $V_{\text{TH}}$ ) measured through  $I_{\text{DS}}^{1/2}-V_{\text{GS}}$  plot was found to be 16.2 V. The irradiated sample shows a significant variation in the electrical characteristics of the OFET. Figure 2(b) shows the transfer characteristics of the irradiated OFET. Here, the OFF current increases with increased dose of irradiation as can be seen in Fig. 2(c). At the same time, decrease in the ON current can be observed in Fig. 2(b). Also, due to a positive charge buildup in the silicon dioxide due to ionizing radiation, negative shift in the threshold voltage<sup>16,17</sup> of the device can be observed from Fig. 2(b). Various parameters such as OFF current ( $I_{\text{OFF}}$ ), ON/OFF current ratio ( $I_{\text{ON}}/I_{\text{OFF}}$ ),

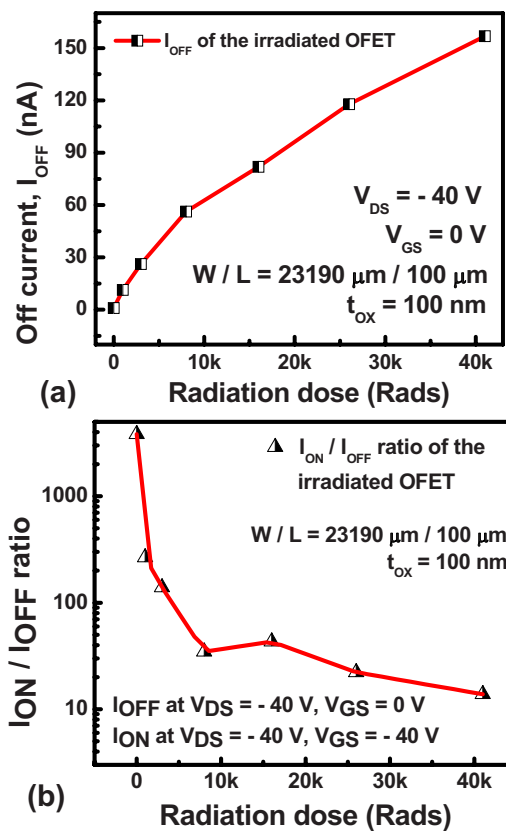


FIG. 3. (Color online) (a) OFF current degradation of the OFET ( $W/L = 23190 \mu\text{m}/100 \mu\text{m}$ ,  $t_{\text{ox}} = 100 \text{ nm}$  and P3HT as *p*-type semiconductor). There is a change of about 150 $\times$  in the  $I_{\text{OFF}}$  after a 41 krad ionizing radiation dose using a  $^{60}\text{Co}$  radiation source. (b) Degradation in  $I_{\text{ON}}/I_{\text{OFF}}$  ratio of the OFET ( $W/L = 23190 \mu\text{m}/100 \mu\text{m}$ ,  $t_{\text{ox}} = 100 \text{ nm}$  and P3HT as *p*-type semiconductor). There is a change of about 300 $\times$  in the  $I_{\text{ON}}/I_{\text{OFF}}$  ratio with 41 krad ionizing radiation dose using a  $^{60}\text{Co}$  radiation source.

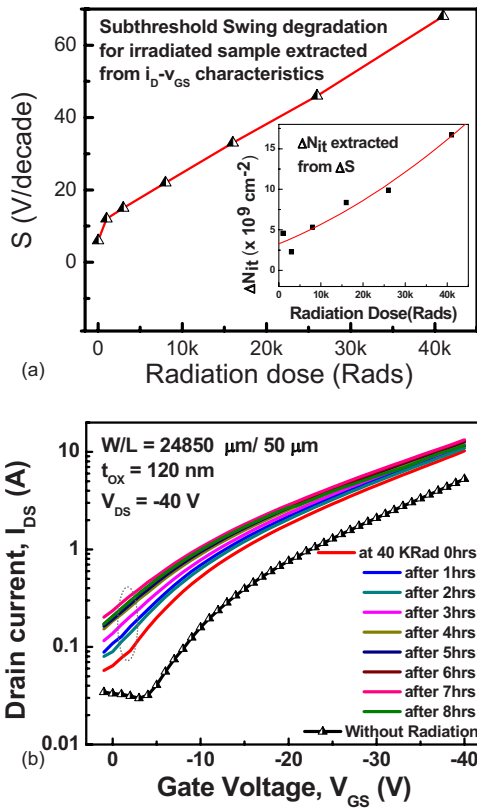


FIG. 4. (Color online) (a) Subthreshold swing degradation in the OFET ( $W/L=23190 \mu\text{m}/100 \mu\text{m}$ ,  $t_{\text{ox}}=100 \text{ nm}$  and P3HT as  $p$ -type semiconductor) with  $^{60}\text{Co}$  radiation dose. The inset figure shows increase in number of interface traps extracted using change in subthreshold swing with increasing ionizing radiation and (b) annealing (time) study on an OFET ( $W/L=24850 \mu\text{m}/50 \mu\text{m}$ ,  $t_{\text{ox}}=120 \text{ nm}$  and P3HT as  $p$ -type semiconductor) subjected to 40 krad ionizing radiation dose of  $^{60}\text{Co}$ .

etc. have been extracted from the measured characteristics after different radiation doses.

Figure 3(a) shows the increase in the OFF current of the device after each dose of radiation. The sample, which was irradiated with  $^{60}\text{Co}$  with the shown dose-rate, exhibits a much higher increase in the OFF current (about six times), starting from a few nanoamperes to hundreds of nanoamperes. As shown in Fig. 3(a), the OFF current increase of the irradiated sample is proportional to the radiation dose. Figure 3(b) shows a plot of ON/OFF current ratio ( $I_{\text{ON}}/I_{\text{OFF}}$ ) with increasing radiation dose. The ratio degrades rapidly in the sample upon irradiation due to a significant degradation in the off current as can be seen in Fig. 2(c) and in the ON current as shown in Fig. 2(b).

Degradation in the subthreshold swing of an OFET is extracted from Fig. 2(c) for subsequent radiation doses. The subthreshold swing increases almost linearly with subsequent radiation doses as shown in Fig. 4(a). The change (increase) in the number of interface states ( $\Delta N_{\text{it}}$ ) can be easily calculated from the change in subthreshold swing,  $\Delta S$ , assuming that the generated interface states are uniformly spread over the band gap. Equation (1) shows a relationship between  $\Delta N_{\text{it}}$  and change in subthreshold swing ( $\Delta S$ ),

$$\Delta N_{\text{it}} = \frac{C_{\text{ox}} \epsilon_g \Delta S}{kT (\ln 10)}. \quad (1)$$

Here, band gap ( $\epsilon_g$ ) for P3HT can be taken as the difference between the HOMO and LUMO. Reported  $\epsilon_g$  values for

P3HT vary between 1.9 to 2.1 eV.  $\epsilon_g=2.1 \text{ eV}$  for P3HT is used in this work for calculation of  $\Delta N_{\text{it}}$ . Calculated  $\Delta N_{\text{it}}$  values are plotted in the inset of Fig. 4(a). To verify that the changes in the electrical characteristics of an OFET due to irradiation are permanent in nature, an annealing study was done on an OFET sample. The sample was irradiated for 40 krad dose with  $^{60}\text{Co}$  radiation. The time dependent annealing characteristics are shown in Fig. 4(b) indicating that the effects are not transient in nature. Here the slight degradation in the characteristics was due to the effect of moisture and oxygen on P3HT film as the sample was kept open in the atmosphere. As has been shown by us earlier, this degradation can be reduced by about 400% with a proper passivation technique.<sup>18</sup> As the oxygen and humidity degrades the semiconductor, the entire study is performed with a nonirradiated sensor sample, which is kept in the same ambient as the irradiated sample and characterized along with the irradiated sample. From the characterized data it can be observed that the degradation in the characteristics due to oxygen and humidity in the atmosphere is less than 10% of the change due to irradiation.

In conclusion, we have explored the use of organic semiconductor transistors for determining the ionizing radiation by experiments. ON current degrades by about 2 $\times$ , OFF current increases by about 150 $\times$  giving rise to an ON/OFF current ratio change, which is by a factor of 300 $\times$  after a total dose of 41 krad. Significant changes are observed in electrical characteristics of irradiated OFETs, suggesting the possibility for use of OFETs as excellent sensors for radiation applications. Using these techniques a real time, active or passive dosimeter can be realized. Organic radiation sensors will have all the advantages of organic electronics such as large area coverage, structural flexibility, and simpler processing resulting in a low production cost.

- <sup>1</sup>L. Adams and A. Holmes-Siedle, *IEEE Trans. Nucl. Sci.* **25**, 1607 (1978).
- <sup>2</sup>N. Bhat and J. Vasi, *IEEE Trans. Nucl. Sci.* **39**, 2230 (1992).
- <sup>3</sup>L. J. Asensio, M. A. Carvajal, J. A. Lopez-Villanueva, M. Vilches, A. M. Lallena, and A. J. Palma, *Sens. Actuators, A* **125**, 288 (2006).
- <sup>4</sup>D. Braun and A. J. Heeger, *Appl. Phys. Lett.* **58**, 1982 (1991).
- <sup>5</sup>C. J. Brabec, C. Winder, N. S. Scriciftci, J. C. Hummelen, A. Dhanabalan, P. A. van Hal, and R. A. J. Janssen, *Adv. Funct. Mater.* **12**, 709 (2002).
- <sup>6</sup>K. Tsukagoshi, J. Tanabe, I. Yagi, K. Shigeto, K. Yanagisawa, and Y. Aoyagi, *J. Appl. Phys.* **99**, 064506 (2006).
- <sup>7</sup>T. W. Kelley, L. D. Boardman, T. D. Dunbar, D. V. Muires, M. J. Pellerite, and T. P. Smith, *J. Phys. Chem. B* **107**, 5877 (2003).
- <sup>8</sup>C. D. Dimitrakopoulos and P. R. L. Malenfant, *Adv. Mater. (Weinheim, Ger.)* **14**, 99 (2002).
- <sup>9</sup>H. Klauk, M. Halik, U. Zschieschang, F. Eder, D. Rohde, G. Schmid, and C. Dehm, *IEEE Trans. Electron Devices* **52**, 618 (2005).
- <sup>10</sup>D. A. Thomas, B. J. Debeurre, and P. J. Thoma, U.S. Patent No. US 7, 141,839, B2 (2006).
- <sup>11</sup>H. Wohltjen, U.S. Patent No. US 4, 572, 900 (1986).
- <sup>12</sup>P. E. Keivanidis, N. C. Greenham, H. Sirringhaus, R. H. Friend, J. C. Blakesley, R. Speller, M. Campoy-Quiles, T. Agostinelli, D. D. C. Bradley, and J. Nelson, *Appl. Phys. Lett.* **92**, 023304 (2008).
- <sup>13</sup>T. Agostinelli, M. Campoy-Quiles, J. C. Blakesley, R. Speller, D. D. C. Bradley, and J. Nelson, *Appl. Phys. Lett.* **93**, 203305 (2008).
- <sup>14</sup>G. Zotti and S. Zecchin, *Synth. Met.* **87**, 115 (1997).
- <sup>15</sup>Z. Wei, J. Xu, S. Pu, and Y. Du, *J. Polym. Sci., Part A: Polym. Chem.* **44**, 4904 (2006).
- <sup>16</sup>P. S. Winokur, H. E. Boesch, Jr., J. M. McGarrity, and F. B. McLean, *J. Appl. Phys.* **50**, 3492 (1979).
- <sup>17</sup>J. A. Felix, J. R. Schwank, D. M. Fleetwood, M. R. Shaneyfelt, and E. P. Gusev, *Microelectron. Reliab.* **44**, 563 (2004).
- <sup>18</sup>S. P. Tiwari, P. Srinivas, S. Shriram, N. S. Kale, S. G. Mhaisalkar, and V. R. Rao, *Thin Solid Films* **516**, 770 (2008).